The cellular mammalian clock regulates *Staphylococcus aureus* invasion in epithelial cells

Pooja Agarwal[1], Giridhar Chandrasekharan[1], Jaspreet Grewal[1], Robert Dallmann[1,2,*] and Meera Unnikrishnan[1,*]

[1] Division of Biomedical Sciences, Warwick Medical School, University of Warwick, Coventry, UK

[2] Zeeman Institute for Systems Biology & Infectious Disease Epidemiology Research (SBIDER), University of Warwick, Coventry, UK

* Corresponding authors

Addresses for correspondence:

r.dallmann@warwick.ac.uk and m.unnikrishnan@warwick.ac.uk

Abstract

An endogenous biological clock, the circadian clock, coordinates life with the 24-hour day/night cycle of the environment. The unit of this circadian clock is the cell but in multicellular organisms, such as mammals, a circadian timing system (CTS) with a central pacemaker orchestrates peripheral clocks and the overall finely tuned temporal order. For example, the CTS changes immune responses to infections depending on time-of-day, however, its role in controlling bacterial infections at a cellular level is not understood.

In this study, we investigated the role of the host cellular clock during infection by *Staphylococcus aureus,* a highly drug-resistant, facultatively intracellular human pathogen. Our findings revealed that *S. aureus* invasion into epithelial cells is dependent on the cellular circadian phase. Interestingly, in BMAL1*,* an essential clock protein, deficient cells bacterial uptake was significantly higher compared to parental A549 cells. RNA sequencing of *BMAL1* knockdown (KD) cells showed a significant upregulation of *GP340*, coding for the receptor of SraP, an *S. aureus* adhesin. An *S. aureus* mutant lacking SraP did not exhibit a circadian rhythm of uptake into A549 cells nor an increased uptake into *BMAL1* KD compared to the parental A549 cells. Of note, bacterial mutants for other adhesins continued to show a rhythmic and higher uptake in *BMAL1* KD cells.

Hence, we report that *S. aureus* invasion of epithelial cells is clock-modulated and mediated through *S. aureus* SraP, suggesting potential for host clock-directed therapy against this pathogen.

40 **Introduction**

41 Circadian rhythms are intrinsic, about 24-hour cycles that govern a wide array of
42 physiological processes in most living organisms, ranging from bacteria to humans [1,2].
43 These rhythms are regulated by a cell autonomous internal time-keeping system
44 known as the circadian clock, which allows organisms to anticipate and adapt to daily
45 environmental changes, synchronize metabolic functions, and maintain overall
46 homeostasis [3].

47 In mammals, a central clock in the hypothalamic suprachiasmatic nucleus (SCN)
48 coordinates rhythms in all other organ, tissue and cellular clocks relative to the
49 environmental light/dark cycles. The molecular basis of circadian rhythms involves
50 coupled transcriptional-translational feedback loops consisting of more than a dozen
51 core clock genes[1], including the central positive and negative arm transcription factors
52 BMAL1, CLOCK and PERIODs, CRYPOTCHROMEs, respectively. These genes
53 interact to produce proteins that oscillate in abundance over an approximate 24-hour
54 cycle, ultimately regulating downstream processes involved in metabolism, immunity,
55 inflammation and various physiological responses[4,5].

56 Recent research has underscored the significant influence of the circadian clock on
57 immune regulation and host-pathogen interactions[6]. The synchronization between the
58 circadian system and immune responses ensures that the body can efficiently combat
59 pathogens at optimal times of the day[7,8]. For example, studies have shown that
60 immune cells exhibit diurnal variations in activity, with certain populations peaking at
61 specific times, thereby enhancing the body's ability to respond to infections[9].
62 Disruptions to circadian regulation, whether due to genetic, environmental, or
63 behavioural factors, can impair these defences, leading to increased susceptibility to
64 infections and altered pathogen behaviour[10,11]. Additionally, dysregulation of the host
65 circadian clock has been linked with increase susceptibility to bacterial infection[12].

66 *Staphylococcus aureus*, a Gram-positive bacterium, is a highly drug resistant
67 opportunistic human pathogen responsible for a wide range of infections, from minor
68 skin conditions to life-threatening diseases such as pneumonia, endocarditis, and
69 sepsis[13,14]. *S aureus* is a facultative intracellular pathogen, which invades a range of
70 mammalian cells, which offer a niche for replication, persistence and resistance to
71 antimicrobials[15-18]. Recent findings suggest that disruption of circadian regulation can

impair immune responses towards *S. aureus* infection[19]. However, at a cellular level, the molecular mechanisms underlying the ole of the host clock in *S. aureus* infection remain unclear. Identifying host pathways involved may lead to the development of chronotherapeutic approaches that optimize timing for interventions against *S. aureus* infections.

In this study, we explore the role of the host circadian clock in modulating *S. aureus* infection of epithelial cells in an *in vitro* infection model. We demonstrate that *S. aureus* invasion is dependent on the mammalian circadian phases and that specific bacterial adhesins may control rhythmic invasion through interactions with clock-regulated host proteins. This study implicates potential molecular targets that could inform new strategies against *S. aureus* infection.

83 **Methods and Materials**

84 **Bacterial strains, plasmids, and bacterial culture conditions**

85 *Staphylococcus aureus* strains, *S. aureus* JE2 wild-type (WT) (BEI Resources),
86 including *S. aureus* reporter strains (containing pMV158-mCherry or pMV158-GFP),
87 *S. aureus*::mCherry (pOS1), *S. aureus*::GFP (pMV158), were cultured in tryptic soy
88 broth (TSB) medium at 37°C with shaking, in the presence or absence of 5 µg/mL
89 tetracycline, as appropriate.

90 Transposon mutants of key adhesion factors, including FnbA (fibronectin-binding
91 protein A), FnbB (fibronectin-binding protein B), and SraP (serine-rich adhesin for
92 platelets), were obtained from BEI Resources. These mutants were handled and
93 maintained according to the manufacturer's instructions to preserve their genetic
94 integrity and viability for subsequent experiments.

95 For infection experiments, bacterial cultures were initiated a day before the assay by
96 inoculating were grown overnight cultures from frozen stocks. These overnight
97 cultures were prepared to ensure bacterial viability and consistency. On the day of the
98 experiment, log-phase cultures were initiated by diluting the overnight cultures into
99 fresh TSB medium. Bacteria were grown in a shaker at 37°C to an optical density at
100 600 nm (OD_{600}) of 1.0, indicating active growth in the exponential phase of bacterial
101 growth.

102 **Mammalian cell culture and circadian synchronization**

103 Human lung epithelial A549 cells wild type (ATCC CCL-185) with or without sh*BMAL1*
104 knockdown were cultured in DMEM supplemented with GlutaMAX™ (ThermoFisher
105 Scientific), 1% Penicillin/Streptomycin and 10% fetal bovine serum (FBS). Cells were
106 maintained in a humidified atmosphere at 37°C with 5% CO_2.

107 To evaluate *Staphylococcus aureus* invasion, mammalian cells were seeded in 24-
108 well plates or four-chambered slides at a density of 3×10^5 cells per well and incubated
109 for 24 hours prior to infection.

110 For circadian synchronization experiments, cells were seeded at a density of 2×10^5
111 cells per well and allowed to adhere for 24 hours. Synchronization was achieved using
112 forskolin (FSK, 10 µg/mL), a potent cyclic AMP (cAMP) activator known to reset the

113 circadian clock of all cells in the culture vessel to a common phase [20,21]. Cellular clocks
114 were reset 6, 12, 18, or 24 h before infection with *S. aureus* to assess circadian phase
115 difference of bacterial invasion (Figure 1A).

116 For microscopy-based assessments, cells were seeded either in imaging 24-well
117 plates (Greiner) or on four-chambered slides (Nunc, Lab-Tek II) to facilitate imaging of
118 *S. aureus* interactions with epithelial cells.

119 **Generation of transgenic A549 cell lines**

120 *BMAL1* knockdown cells were generated by lentiviral transgenesis following a
121 published strategy[22]. In short, lentiviral particles were generated by transfection of
122 HEK293FT cells (Invitrogen) with a third generation lenti-viral backbone pGIPZ for
123 *shBMAL1* packaging and capsid plasmids (pCMVR8.74 and pMD2.G) using Trans-it
124 lentivirus reagent (Mirrus Bio) as described[23]. Viral supernatant was sterile filtered and
125 frozen at -80ºC until use. For lentiviral transduction, viral supernatant with 8 µg/mL
126 polybrene was added onto 60% confluent A549 cells, and incubated at 37ºC for 6 h,
127 after which cells were washed and incubated for 3 days in standard media. Afterwards,
128 media was supplemented with 10 µg/ml puromycin to select infected cells. Co-
129 expressed eGFP was assessed as further confirmation that cells had integrated the
130 *shBMAL1* construct.

131 **Invasion and survival assays**

132 To evaluate the invasion of A549 cells, *S. aureus* cultured to OD_{600} of 1.0 (logarithmic
133 growth phase) were harvested by centrifugation at 5000 xg for 10 minutes and washed
134 twice with phosphate-buffered saline (PBS). The bacterial pellet was resuspended in
135 PBS and the required volume of this culture was added to the cell culture medium to
136 prepare the inoculum; 3×10^6 or 6×10^6 CFU/ml. This inoculum was added to epithelial
137 cells for 1 h to achieve a multiplicity of infection (MOI) of 10:1. Following the infection
138 period, extracellular bacteria were removed by incubating cells in culture medium
139 containing gentamicin (50 µg/mL) and lysostaphin (20 µg/mL) for 30 minutes. The
140 cells were then washed three times with PBS and lysed with cold water to release
141 intracellular bacteria. To enumerate colony forming units (CFU), cell lysates were
142 serially diluted and plated onto tryptic soy agar (TSA; Sigma). To monitor the
143 intracellular growth kinetics of bacteria using microscopy, infected cells were

144 incubated with 2 µg/mL lysostaphin. Imaging was performed using either a BioTek
145 Cytation 5 Multimode Reader (Agilent) or a confocal microscope (Olympus FV3000).

146 Analysis of rhythmic patterns for synchronised cells infected with *S. aureus* was
147 conducted on bacterial CFU or the fold-changes of internalised bacterial CFU/ml
148 (bacterial invasion) relative to unsynchronised cells. A COSINOR model was used as
149 previously described [24], using the equation Y=(Mesor+Amplitude*cos(((2*pi)*(X-
150 Acrophase))/Period)) with constraining Period to over 20 h. The linear model was Y=
151 YIntercept + X*Slope with no further constraint. Data was fit to COSINOR and linear
152 models and an extra sum-of-squares F-test was run at $p<0.01$ with the linear model
153 as null hypothesis.

154 **RNA-Seq and data analysis**

155 To harvest RNA, parental and *shBMAL1* A549 cells were seeded and synchronised
156 by FSK as described above. RNA was extracted at the indicated times post
157 synchronisation using the RNeasy Plus kit (Qiagen, 74134). Briefly, the cells were
158 washed thrice in PBS and lysed in the RLT buffer from the kit. Genomic DNA was
159 removed from the lysate using a gDNA eliminator spin column from the kit. 1 volume
160 of 70% ethanol was added to the flowthrough and loaded on a RNeasy spin column.
161 The column was centrifuged at 8000 xg for 30 s. This was followed by subsequent
162 washes with RW1 and RPE buffer. Excess ethanol from the column was removed by
163 spinning the column at 13000 xg for 1 min. Twenty ml RNase free buffer was added
164 to the column and spun at 8000 xg for 1 min. RNA was quantified using the Qubit
165 assay. The RNA samples (30 ng/µl) were sent to Novogene for library preparation
166 after poly(A) enrichment and subsequently sequenced using a pair-ended 150 bp kit
167 on an Illumina NovaSeq. Sequencing depth was at least 15 million reads per sample.
168 Gene count tables were generated using Kallisto on the BioJupies platform[25]. All
169 further analysis was conducted using iDEP 2.0[26]. The DESeq2 algorithm was used for
170 differential gene expression analysis with FDR cutoff of 0.01. Variance stabilising
171 transformation was used for PCA, heatmap and single gene visualisations and gene
172 expression reporting. Parametric Gene Set Enrichment Analysis (PGSEA) of KEGG
173 pathways was used for pathway analysis with FDR cutoff of 0.0001[27]. RNA-Seq data
174 are available at the ELIXIR database ArrayExpress under accession number E-MTAB-
175 15036.

176 **Western blotting**

177 To prepare cell lysates, synchronized and non-synchronised cells were lysed using
178 RIPA buffer. Samples were separated on a 4-12% Native-PAGE gel and then
179 transferred onto a nitrocellulose membrane (Bio-Rad). The membrane was blocked
180 for 1 hour with 5% non-fat milk and then incubated overnight at 4°C with 1 mg/ml anti-
181 BMAL1 mAb (Abcam, 93806), diluted 1:2000. Membranes were washed three times
182 with Tris buffered saline with 0,1% Tween-20 (TBS-T) and incubated with a 1:2000-
183 diluted HRP-conjugated secondary goat anti-mouse antibody (Abcam, 205718)) for 1
184 hour at room temperature (RT). After washing three times with TBS-T, the signal was
185 detected using ECL Western Blot Substrate according to the manufacturer's
186 instructions.

187 The blot was then stripped using stripping buffer, washed with TBS-T, blocked again
188 for 1 hour with TBS containing 5% non-fat milk, and incubated overnight at 4°C with 1
189 mg/ml anti-Actin mAb, diluted 1:2000. The next day, membranes were washed three
190 times with TBS-T and incubated with a 1:2000-diluted HRP-conjugated secondary
191 goat anti-mouse antibody (Abcam, ab8227) for 1 h at RT followed by detection with
192 ECL substrate as above.

193 **Microscopy and image analysis**

194 Image analysis for data recorded on the Cytation 5 was conducted using the BioTek
195 Gen5 software. For live cell microscopy, for each sample, a region of interest (ROI)
196 was identified and tracked over a 24 h period.

197 For bacterial visualization via confocal microscopy, cells were fixed with 4%
198 paraformaldehyde (PFA) for 1 hour, followed by three washes with PBS. Actin was
199 stained with Phalloidin 650 in the dark for 1 h. After staining, cells were washed three
200 times with PBS, air-dried, and mounted using a mounting medium containing DAPI for
201 nuclear staining. Stained samples were observed using an Olympus FV3000 Confocal
202 Laser Scanning Microscope. Images were analysed with ImageJ using Fiji.

203 **Results**

204 ***S. aureus* invasion of human lung epithelial cells is dependent on circadian**
205 **phase**

206 To investigate the role of the circadian clock in the invasion of *S. aureus*, A549 cells
207 were synchronized using forskolin, a well-known natural compound commonly
208 employed for cellular clock synchronization[21]. Epithelial cells were synchronised by
209 forskolin at six-hourly intervals over a 24 h period and subsequently infected with
210 *S. aureus* for 1 h. In addition, unsynchronised A549 cells were infected (Figure 1A).
211 Notably, compared to unsynchronised cells, a higher number of intracellular bacteria
212 was observed in synchronised cells after 12 h hours before infection, as measured by
213 colony forming units (CFU), whereas a significantly lower uptake was detected in cells
214 synchronised 24 h before infection. These findings suggest that the phase of the
215 cellular circadian clock modulates the uptake of *S. aureus* (Figure 1B). Non-linear
216 curve fitting COSINOR analysis suggested a significant rhythmicity with and
217 approximately 3-fold change in colony-forming units (CFU) between the 12 h and 24 h
218 samples (Figure 1C).

219 To verify this result and visualize intracellular bacterial foci, confocal microscopy was
220 performed on fixed samples infected at different circadian phases as above. We found
221 a higher number of intracellular bacteria within cells synchronised 12 h before infection
222 compared to those 24 h before. Quantification of these samples showed on average
223 of ~3 bacterial foci per 100 mammalian cells in 12 h after FSK synchronisation, while
224 this decreases at 24 h post FSK to 1.5 bacterial loci foci per 100 mammalian cells
225 (Figure 1E), reinforcing the notion that the host's circadian clock may play a modulating
226 role in bacterial uptake with an amplitude of 2-3-fold.

227 We further monitored the intracellular growth kinetics of *S. aureus* in the presence of
228 5 µg/ml lysostaphin, which kills extracellular bacteria (Figure S1A) for 12 h after
229 infection of A549 cells using fluorescence live-cell imaging. As above, synchronised
230 A549 cells were infected at four distinct circadian phases. Consistent with results for
231 invasion, our data showed a steeper increase in bacterial foci in the earlier time (6 h
232 and 12 h) and a longer time to reach peak intra-cellular bacterial load (Figure S1B).

233 Together our findings highlight a potential role for the circadian clock in modulating
234 mammalian host cell factors for *S. aureus* cell invasion.

235

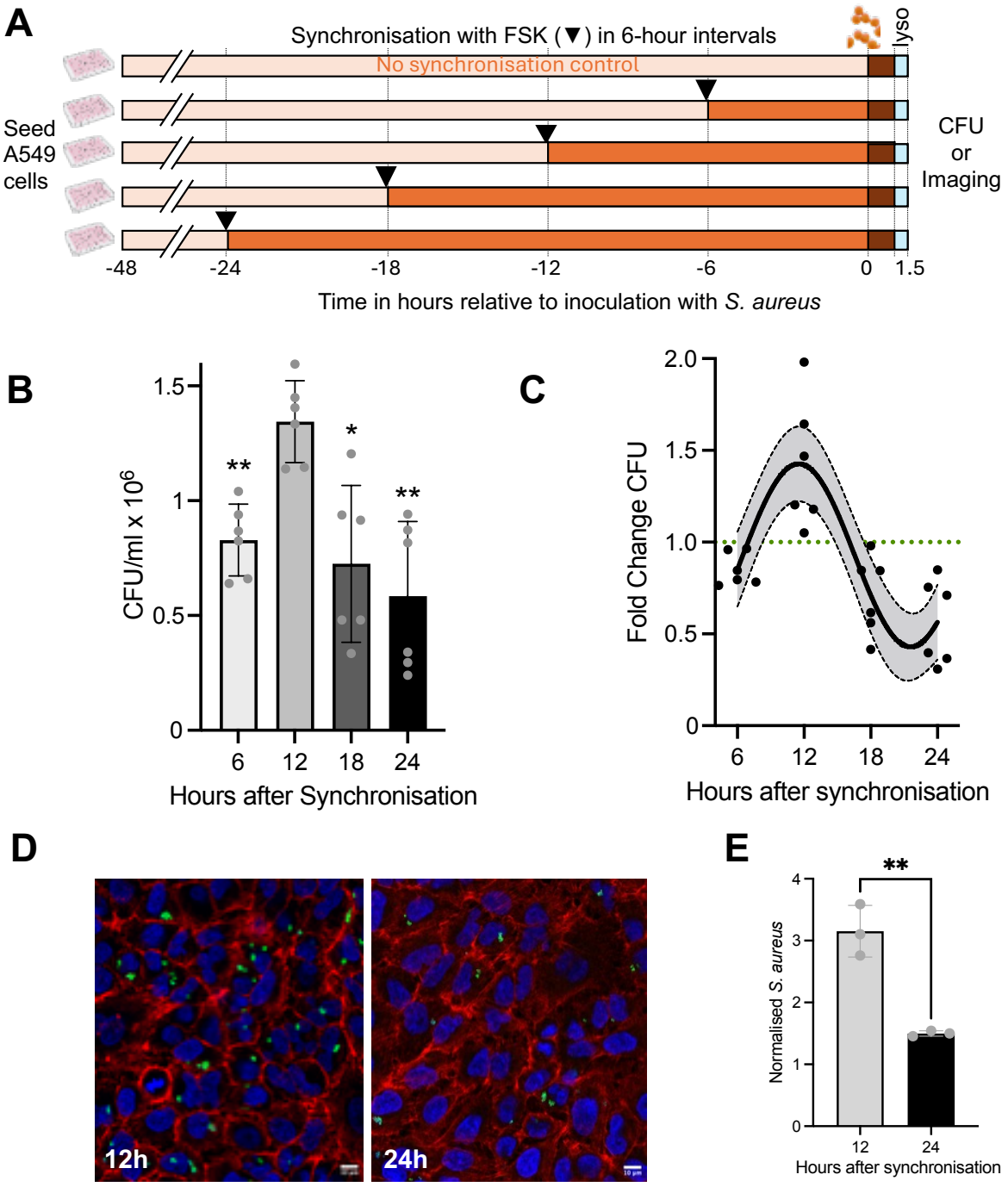

236

237 ***Figure 1. S. aureus invasion is modulated by epithelial cell circadian phase.*** *(A)*
238 *Schematic diagram showing experimental design. A549 cells were synchronized with*
239 *forskolin (FSK) every 6 h for a 24 h period. FSK synchronised or unsynchronised cells*
240 *were infected with wildtype JE2 S. aureus for 1 h, and extracellular bacteria were*

241 *removed by gentamycin/lysostaphin treatment. (B) Intracellular bacterial numbers*
242 *determined by colony counts (CFU) from different times after synchronisation (green*
243 *dashed line shows value for mean unsynchronised cells), mean ± SD, significant*
244 *ANOVA with post-hoc comparison to 12 h point indicated by * p>0.05 and ** p<0.01,*
245 *N=6. (C) Data from B plotted as fold-change in CFU compared to an unsynchronized*
246 *control showing COSINOR best fit with 95% confidence interval. (D) Confocal images*
247 *of epithelial cells, synchronized by FSK for 24 h and 12 h, green - foci of intracellular*
248 *S. aureus-GFP, Red - actin stained by Phalloidin Alexa flour 647, Blue - nuclei stained*
249 *by DAPI.) Number of bacterial foci (green) and the number of cell nuclei (blue) in cells*
250 *synchronized for 12 and 24 h were counted manually- 5 fields were counted from 3*
251 *independent experiments, mean ± SD, p = 0.003, unpaired t-test.*

252

253 **Rhythmic *S. aureus* invasion is lost in clock-disrupted human epithelial cells**

254 To investigate if the observed changes are driven by the canonical circadian clock, we
255 generated clock-disrupted A549 cells by targeting the transcription factor BMAL1, an
256 essential core circadian clock gene[1,28]. We generated *BMAL1* knockdown (sh*BMAL1*)
257 A549 cells using a lentiviral transduction system. Successfully transfected cells were
258 selected based on puromycin resistance and presence of the knockdown-construct in
259 the cells was confirmed by eGFP expression (Figure S2A). Downregulation of BMAL1
260 protein expression was confirmed via western blot analysis (Figure 2A). Quantitative
261 densitometric analysis of the blots revealed a 50% reduction in BMAL1 protein levels
262 in knockdown cells compared to parental A549 cells (Figure 2B). Gene expression
263 profiling with RNA-Seq also confirmed downregulation of *BMAL1* mRNA and pathway
264 analysis suggested a disruption of the KEGG pathway for “circadian rhythm” (Figure
265 S2B, C).

266 We then tested the clock disrupted *shBMAL1* A549 cells in the infection assay with
267 *S. aureus* as described above. Unlike parental cells, which again exhibited a circadian
268 phase-dependent rhythm of bacterial invasion, a temporal invasion pattern was
269 abolished in *shBMAL1* A549 cells. Non-linear COSINOR fit the data statistically worse
270 (Sum-of-squares F-test) than a linear model for *shBMAL1* cells (Figure 2D). This
271 observation strongly suggests the circadian clock, for which *BMAL1* is a critical
272 regulator, is necessary for *S. aureus* invasion rhythms in A549 cells.

273

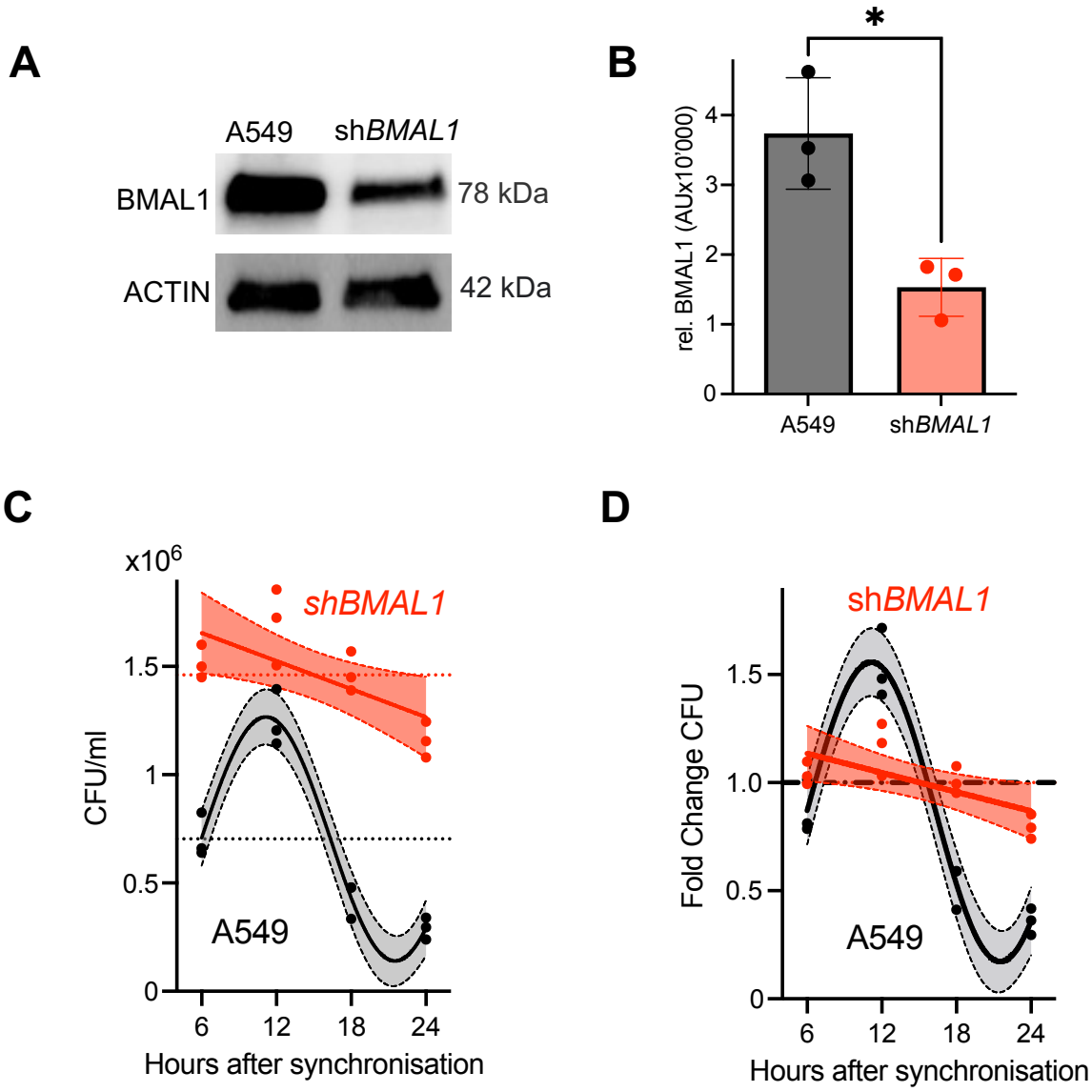

274

275 ***Figure 2. The canonical circadian clock is necessary for rhythm of S. aureus***
276 ***invasion.*** *(A) Western blot of parental and shBMAL1 A549 cell lysates confirms*
277 *BMAL1 knockdown. (B) Quantitation of band intensities relative to ACTIN showed an*
278 *approximately 2-fold reduction, N = 3, *p = 0.0166, unpaired t-test. (C & D) Time-series*
279 *of S. aureus invasion in parental (black: A549) and shBMAL1 (red: shBMAL1) A549*
280 *cells as described in Figure 1. Dotted lines on graph show the level of infection of*
281 *unsynchronized control cells of each cell line. Best fit for COSINOR or linear model*
282 *show depending on sum-of-squares F-Test as described in methods section.*

283

284 Interestingly, our data in *shBMAL1* A549 cells suggests an increase in *S. aureus*
285 invasion irrespective of time after synchronization. Quantitative CFU analysis showed
286 that the uptake in knockdown cells was approximately 1.7-fold higher than in parental
287 A549 cells (Figure 3A). Furthermore, intracellular bacterial survival after 4 hours was
288 also higher for *shBMAL1* cells (Figure 3B). To visualize intracellular bacteria, we
289 performed confocal microscopy on fixed mammalian cells. Consistent with the CFU
290 data, microscopy images confirmed a greater number of intracellular bacterial foci in
291 sh*BMAL1* cells compared to the parental line (Figure 3 C, D). The significantly higher
292 bacterial burden in *BMAL1* knockdown cells highlights its role as a regulator of host-
293 pathogen interactions, potentially through pathways that influence cellular processes
294 such as bacterial recognition, adhesion, or uptake.

295

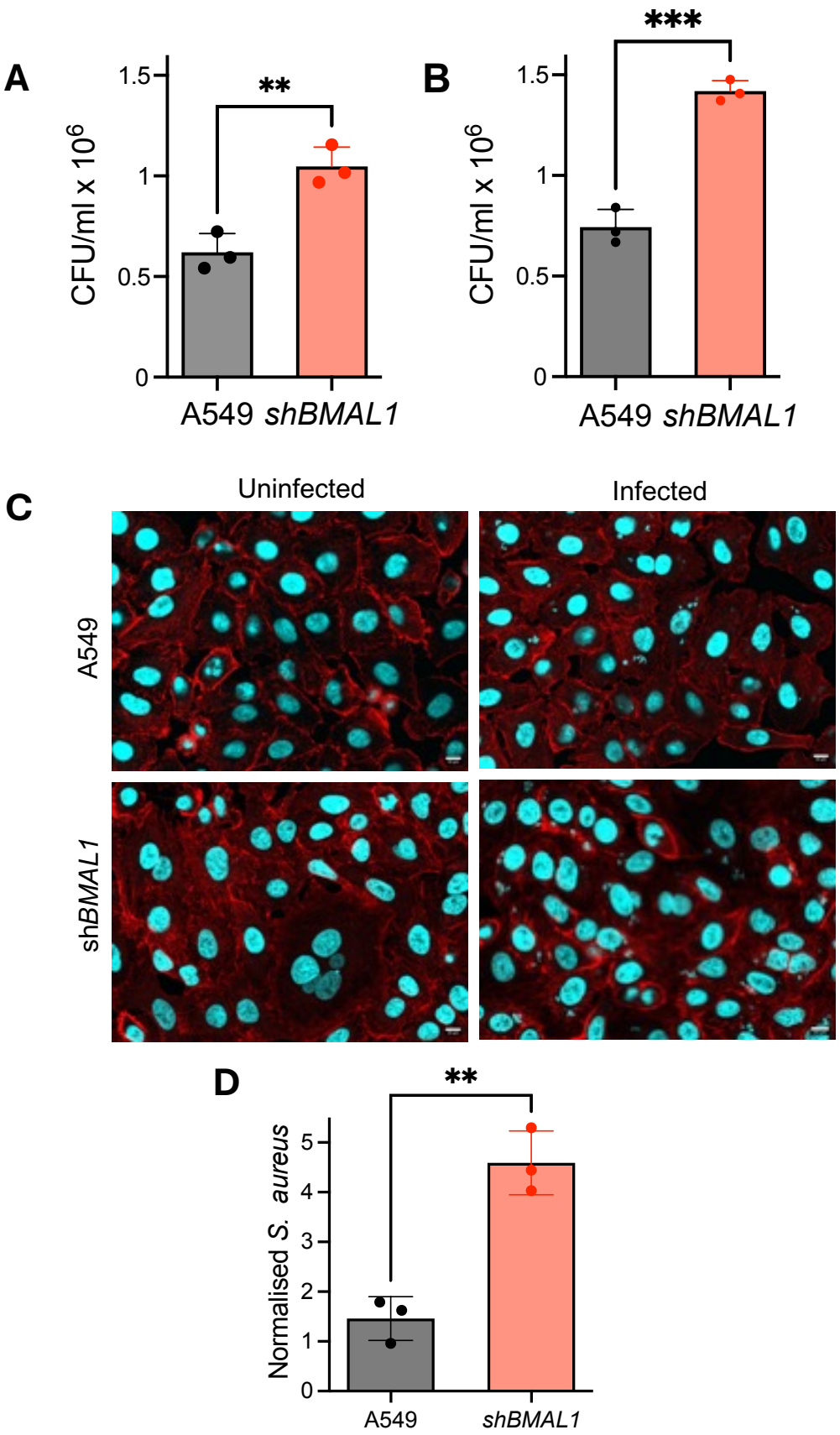

296

297 ***Figure 3. Clock-disrupted cells are more permissive for S. aureus invasion.*** *(A)*

298 *Parental and shBMAL1 A549 cells were infected with S. aureus JE2 as described in*

299 *Figure 1, but after extracellular bacteria were removed cells were further incubated for*
300 *24 h in the presence of lysostaphin. Intracellular bacterial counts after (A) 1 h and (B)*
301 *24 h post infection. N=3, mean+/-SD, **p < 0.01, ***p < 0.001, unpaired t-test. (C)*
302 *Merged confocal images from infected and un-infected cells 24 h after infection, Red-*
303 *actin stained by Phalloidin Alexa flour 647, Blue- bacterial DNA and cell nuclei stained*
304 *by DAPI. (D) Quantification of intracellular bacterial number relative to number of*
305 *mammalian cells from confocal images with at least 5 fields of view per independent*
306 *experiment, N=3, p = 0.0022, unpaired t-test.*

307

308 **Effects of sh*BMAL1* knockdown on the lung epithelial cell transcriptome**

309 To investigate the potential mechanisms underlying the increased bacterial uptake
310 after infection with *S. aureus* 12 h versus 24 h post synchronisation and the time-
311 invariant increase in sh*BMAL1* knockdown cells, we sequenced the transcriptome of
312 parental and sh*BMAL1* lines at 12 h and 24 h post synchronisation. The resulting
313 principal component analysis indicated good separation by cell line (significant
314 correlation with PC1, p = 9.75e-07, Figure 4A). Comparing both cell line samples from
315 12 h & 24 h together, using DESeq2 we found 1773 higher and 1920 genes
316 significantly lower expressed in knockdown vs. parental cells. Furthermore, 29 and
317 three genes were significantly down or up-regulated, respectively at 12 h compared to
318 24 h post FSK, and no DEGs were found for the interaction term of cell line and timing.
319 Given the low number of samples, this was not unsurprising. However, pathway
320 analysis using PGPSEA indicated that 17 KEGG pathways were significantly enriched
321 (Figure 4B). Reassuringly, “circadian rhythms” was significantly less active in the
322 knockdown cells (Figure 4B, Figure S2). Of the other 16 pathways, at least half have
323 some relevance with infection and inflammation processes. Interestingly, “*S. aureus*
324 infection” being one of them (Figure 4B).

325 Contrary to expectations, we did not observe consistent changes in the expression of
326 genes encoding integrins α5 and β1, the receptors to which S*. aureus* adhesins
327 fibronectin binding proteins, Fnbp A and Fnbp B, bind to for the invasion of epithelial
328 cells[29,30]. The gene encoding for *ITGA5* was not significantly changed, and *ITGB1* was
329 even significantly downregulated (Figure 4C). However, when we systematically

330 assessed all integrin isoforms and other extracellular proteins known to be involved in
331 *S. aureus* invasion, we found several other integrin isoforms like *ITGB2*, *ITGB5* were
332 upregulated in the *shBMAL1* A549 cells (Figure 4). Most interestingly, we observed a
333 substantial upregulation of the *GP340* coding gene (a.k.a. *DMBT1*). The bacterial
334 ligand to GP340 is the *S. aureus SraP* protein, which has been reported to facilitate
335 bacterial uptake [31,32]. Thus, regulation of *GP340* in the clock-deficient A549 cells may
336 be important in the circadian modulation of *S. aureus* uptake.

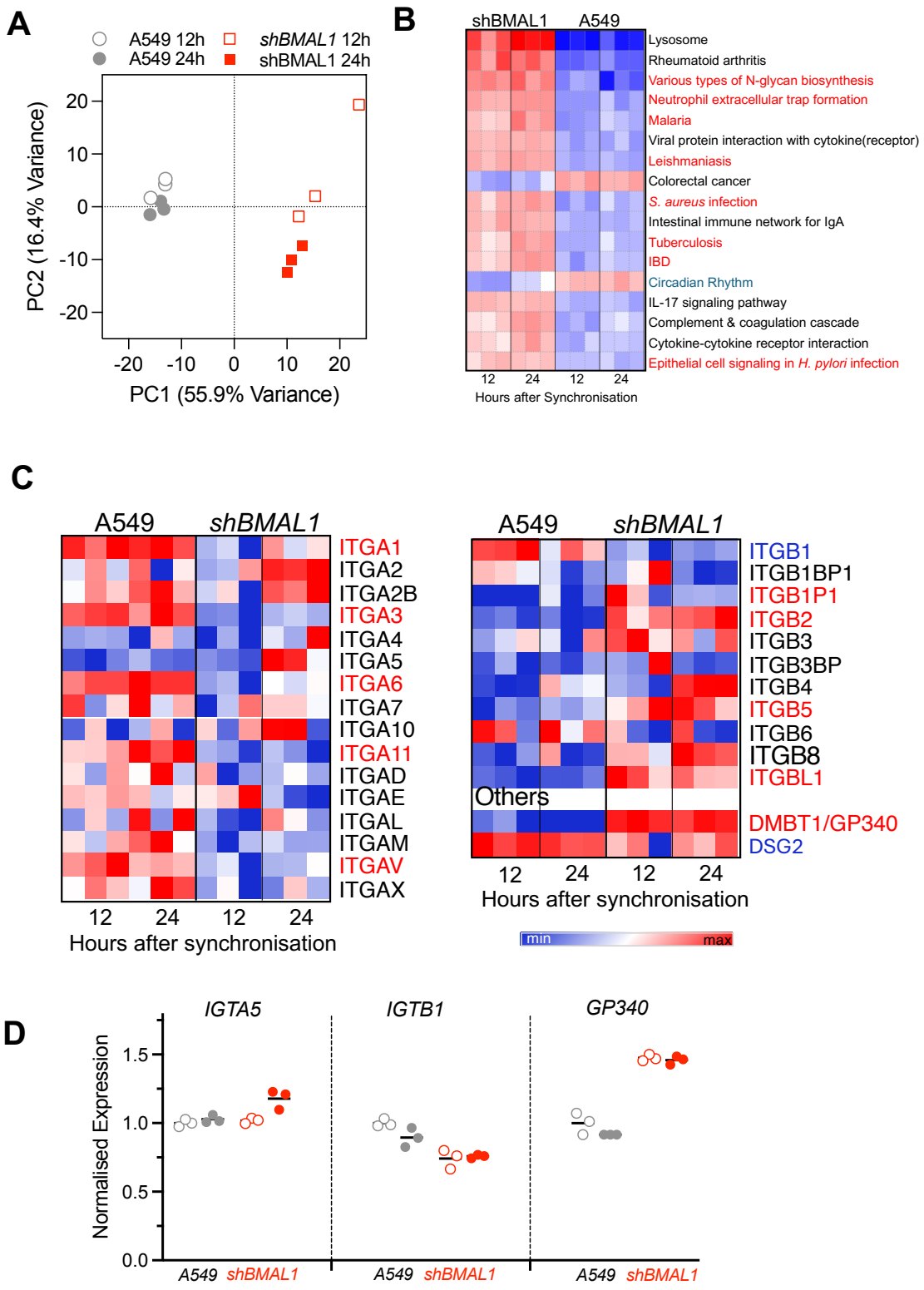

337

338 ***Figure 4. BMAL1 knockdown cells exhibit significant changes in gene***
339 ***expression.*** *(A) PCA plot comparing the variance in gene expression by RNA-Seq*
340 *between parental and shBMAL1 A549 cells collected at 12 h and 24 h after*

synchronisation. (B) Significantly regulated KEGG pathways by PGPSEA analysis. (C) Heatmap showing gene expression profiles for genes encoding integrin A (ITGA) and B (ITGB) subunits and other receptors (DMBT1/GP340) involved in S. aureus uptake profiles in parental and shBMAL1 A549 cells. Names of DEGs in red font. (D) VST normalised expression of IGTA5, IGTB1 and GP340 at 12 h (open circles) and 24 h (closed circles) in parental (grey) and shBMAL1 (red) A549 cells.

The *S. aureus* adhesin *SraP* mediates higher bacterial uptake by sh*BMAL1* cells

To directly test the role of *GP340* in rhythmic *S. aureus* invasion, we compared the internalisation of an *S. aureus sraP* mutant with the WT JE2 strain used above in both, the parental and sh*BMAL1* A549 cells. Consistent with the data shown in Figures 2 and 3, the uptake of *S. aureus* JE2 by sh*BMAL1* knockdown cells was significantly increased compared to parental A549 cells, however, uptake of the s*raP* mutants in *shBMAL1* was similar to that by the parental A549 cells (Figure 5A). Importantly, in both cell lines, and consistent with Figures 1 and 2, JE2 but not s*raP* mutants showed rhythmic invasion in A549 cells. As expected, both strains did not show rhythmic invasion into *shBMAL1* A549 cells (Figure 5B), but a much higher invasion in non-synchronised cells (Figure 5A).

Additionally, we infected both cell types with transposon mutants lacking FnbpA and FnbpB), key *S. aureus* adhesins/invasins. We observed that while the uptake of these mutants was also higher in *shBMAL1* when compared to parental A549 cells, there was no difference when we compared fold changes relative to WT JE2 (Figure S3B).

Thus, in contrast to other adhesins tested, our data suggest that *S. aureus SraP* mediate rhythmic bacterial uptake through GP340 and the observed increase in *BMAL1* knockdown cells.

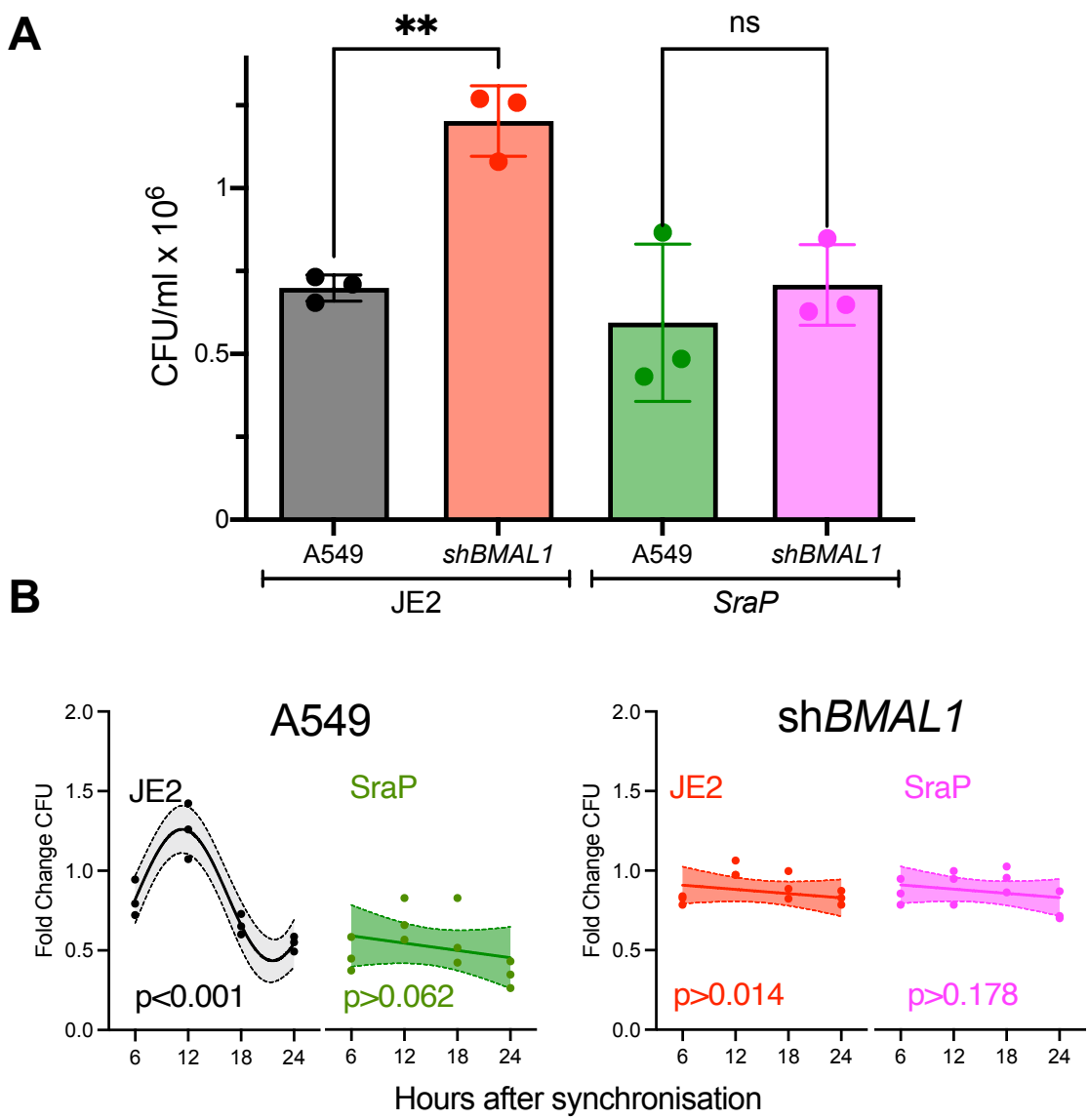

366

367 ***Figure 5. GP340 ligand* SraP *mediates the rhythmic uptake of S. aureus in lung***
368 ***epithelial cells.*** *(A) Parental and shBMAL1 A549 cells were infected with WT*
369 *S. aureus (JE2) or S. aureus sraP transposon mutant for 1 h, and intracellular bacterial*
370 *numbers as measured by CFU were compared. (B) Infection of S. aureus JE2 and*
371 *sraP mutant at four phases of the circadian cycle. Fold changes of CFU for each strain*
372 *to that of respective control unsynchronised cells are plotted. Best fit for COSINOR or*
373 *linear model show depending on sum-of-squares F-Test as described in methods*
374 *section. N = 3.*

375

376 **Discussion**

377 The ability of *S. aureus* to invade and survive within mammalian cells has been
378 attributed to bacterial persistence, antibiotic resistance and recurrent infections.
379 Although *S. aureus* factors that enable cell invasion have been well studied, the host
380 cellular pathways that mediate this are less understood. Circadian rhythms have been
381 demonstrated to influence several host immune responses during infection with some
382 bacteria exhibiting time-of-day differences in infecting flies and mice[12]. However, at
383 the cellular level, the role of the circadian clock in controlling pathogen invasion or
384 intracellular survival is not known. Here we provide evidence for the role of the
385 mammalian circadian clock in modulating invasion of *Staphylococcus aureus* in human
386 lung epithelial A549 cells. We found significant temporal variations in bacterial uptake,
387 a peak in invasion 12 h after forskolin (FSK) synchronisation of the A549 cells and a
388 marked decrease 24 h post synchronisation. Disrupting the clock by a *shBMAL1*
389 knockdown not only abrogated the rhythm in invasion, but also increased the bacterial
390 load, highlighting the influence of the canonical circadian clock in host-pathogen
391 interactions at a cellular level. Notably, using transcriptomic analysis, we identified a
392 significant upregulation of *GP340* in the clock-disrupted *shBMAL1* A549 cells. GP340
393 is a key factor for the uptake of *S. aureus* by epithelial cells, which mediates rhythmic
394 uptake of bacteria through the *S. aureus* adhesin SraP[31-33]

395 Circadian regulation of immune responses is well documented, with evidence
396 suggesting that various immune processes, including cytokine production and
397 phagocytosis, exhibiting circadian variations[34]. Colonisation by bacterial pathogens
398 including *Salmonella typhimurium, Streptococcus pneumoniae and S. aureus* have
399 been shown to be impacted by the time of the day, primarily driven by clock-dependent
400 immune responses to infection[35]. As intracellular survival of many of these pathogens
401 have been reported to be an important feature of bacterial pathogenesis, our findings
402 could be relevant for multiple intracellular pathogens. Our findings extend this
403 knowledge by demonstrating that synchronization with FSK not only impacts the
404 invasion of *S. aureus* but also alters the intracellular responses to bacterial challenge.

405 *BMAL1* has a key role in the regulation circadian rhythms[28]. This complex also
406 activates the transcription of negative regulators, which feedback to inhibit BMAL1-
407 CLOCK activity, ensuring tightly regulated 24-hour rhythms in gene expression[36]. It

408 has been shown that the circadian transcription factor BMAL1 modulates hepatitis C
409 virus (HCV) entry into hepatocytes by regulating the expression of the viral receptors
410 *Cd81* and *Claudin-1*[37]. Pharmacological inhibition of *Bmal1* by REV-ERB agonists
411 reduced *Cd81* and *Claudin-1* expression and inhibited viral entry in cells[37]. Similarly,
412 this was found to down-regulated *angiotensin-converting enzyme 2* expression, which
413 is essential for the entry and replication of SARS-CoV-2 in lung epithelial cells[38]. This
414 highlights the importance of circadian processes for the treatment of viral infection. In
415 addition, various parasitic infections are also linked with regulation of circadian clock[12].
416 Importantly, it has been reported that the complete loss of circadian regulation in
417 *Bmal1* knockdown cells alters the structure of actin cytoskeleton, which is coupled with
418 a significant increase in *S. pneumoniae* burden compared to WT cells, emphasizing a
419 role for *Bmal1* in limiting bacterial uptake and proliferation[39].

420 Our data demonstrated increased bacterial uptake in *BMAL1* knockdown cells
421 occurred independently of FSK synchronization, indicating that the temporal
422 modulation in bacterial uptake cannot be explained by the effect of FSK on cAMP
423 induction per se but establishes a role for *BMAL1* in host susceptibility to *S. aureus*
424 invasion. These observations align with the report that *Bmal1* influences immune cell
425 function and can modulate inflammatory responses[40].

426 Microbial surface components recognizing adhesive matrix molecules (MSCRAMMs)
427 are most prominent surface proteins expressed by staphylococci, which facilitate
428 adhesion to the extracellular matrix (ECM) components such as collagen, fibrinogen,
429 and fibronectin (Fn)[41]. Although, the fibronectin-binding protein (FnBP)–fibronectin
430 (Fn)–α5β1 integrin pathway is the primary route for *S. aureus* internalization[30,42], we
431 did not find upregulation of the main integrins α5β1 in parental vs. *shBMAL1* A549
432 cells. Although *fnbA* and *fnbB* mutants showed reduced uptake in parental cells, they
433 showed higher invasion in *shBMAL1* A549 cells, suggesting involvement of secondary
434 mechanisms in bacterial uptake. As we observed differential regulation of other
435 isoforms of integrins in the RNA-seq, it is possible that other integrin isoforms are
436 potentially involved in bacterial uptake. The specific roles of these isoforms in
437 *S. aureus* uptake, however, have not been extensively studied and their potential
438 involvement in bacterial uptake warrants further investigation.

439 Fibronectin-independent mechanisms are known to mediate *S. aureus* entry and
440 involve distinct surface proteins such as serine-aspartate repeat-containing protein D

441 (SdrD), clumping factor A (ClfA), autolysin (Atl), and serine-rich adhesin for platelets
442 (SraP) [41]. SdrD directly binds Desmoglein 1 (encoded by *DSG1*)[43], ClfA interacts with
443 host cells either directly or via fibrinogen bridges[44] and Atl associates with heat shock
444 cognate protein 70 (*HSPA8*)[45], while SraP binds to the salivary scavenger receptor
445 GP340[31,32]. Interestingly, we found notable upregulation of *GP340* in circadian-
446 disrupted *BMAL1* knockdown cells, and a reduced invasion of *sraP* mutant strains in
447 *BMAL1* knockdown cells suggesting a role for the SraP-GP340 pathway in circadian
448 modulated bacterial invasion. SraP, a member of a family of serine rich glycoproteins
449 encoded by Gram positive bacteria including *Streptococcus spp*[33], was shown to
450 mediate adhesion to epithelial cells through its L-lectin binding module[31]. It was also
451 recently reported to modulate macrophage apoptosis and inflammation, indicating its
452 role in *S. aureus*-immune cell interactions[46].

453 Despite the robust findings of this study, we use of a single epithelial cell line (A549)
454 which may limit the generalizability of the results across different cell types and
455 physiological contexts. Future studies should examine the impact of circadian rhythms
456 on *S. aureus* invasion in other cell types, in particular immune cells may link these
457 findings better to previous studies on circadian effects in immune responses. A
458 broader range of epithelial and immune cell types to ascertain whether similar patterns
459 are observed. Additionally, while our study provides insights into the role of *BMAL1* in
460 regulating bacterial invasion, the specific downstream signalling pathways and
461 molecular mechanisms remain to be elucidated. Further investigation is warranted to
462 dissect these pathways and understand how circadian rhythms influence the
463 expression of key receptors involved in bacterial adhesion and invasion.

464 The implications of these findings extend to the potential for developing therapeutic
465 strategies that target circadian rhythms to improve the timing and efficacy of
466 antimicrobial treatments. For instance, studies have shown that administering
467 antibiotics in alignment with the host circadian cycle can enhance their effectiveness
468 and reduce side effects[47]. In conclusion, our study highlights the critical role of
469 circadian rhythms in modulating the dynamics of *S. aureus* invasion in epithelial cells.
470 Overall, our results highlight the critical interplay between circadian biology and
471 microbial pathogenesis, suggesting that manipulation of circadian pathways may
472 provide new avenues for innovative strategies aimed at preventing and treating
473 bacterial infections.

Acknowledgements

We are grateful for funding from the Warwick Research Development Fund (RD and MU) and a Monash Warwick Alliance fellowship to PA (MU). Anglo American Platinum is gratefully acknowledged for funding work in RDs group.

Author contributions

P.A. designed and carried out the experimental work, analysed the resulting data and co-wrote the manuscript.

G.C. and J.P. contributed to the experimental design, carried out experimental work and contributed to the writing of the manuscript.

R.D. and M.U. jointly supervised the work, and contributed to formal analysis, writing of the manuscript and acquisition of funding.

Competing interests

The authors declare no competing interests.

Data availability

Summary data are depicted in the figures. Raw data are available from the corresponding authors upon reasonable request. RNA-Seq data are available at the ELIXIR database ArrayExpress under accession number E-MTAB-15036.

491 **References**

492 1 Takahashi, J. S. Transcriptional architecture of the mammalian circadian clock.
493 *Nature Reviews Genetics* **18**, 164-179 (2017).
494 2 Wollmuth, E. M. & Angert, E. R. Microbial circadian clocks: host-microbe
495 interplay in diel cycles. *BMC microbiology* **23**, 124 (2023).
496 3 Bass, J. & Takahashi, J. S. Circadian integration of metabolism and energetics.
497 *Science* **330**, 1349-1354 (2010). https://doi.org/10.1126/science.1195027
498 4 Scheiermann, C., Gibbs, J., Ince, L. & Loudon, A. Clocking in to immunity. *Nat*
499 *Rev Immunol* **18**, 423-437 (2018). https://doi.org/10.1038/s41577-018-0008-4
500 5 Shim, D. W. *et al.* Deficiency of circadian clock gene Bmal1 exacerbates
501 noncanonical inflammasome-mediated pyroptosis and lethality via Rev-erbα-
502 C/EBPβ-SAA1 axis. *Experimental and Molecular Medicine* **56**, 370-382 (2024).
503 6 Ponton, F., Wilson, K., Cotter, S. C., Raubenheimer, D. & Simpson, S. J.
504 Nutritional immunology: a multi-dimensional approach. *PLoS Pathog* **7**,
505 e1002223 (2011). https://doi.org/10.1371/journal.ppat.1002223
506 7 Morris, C. J., Purvis, T. E., Hu, K. & Scheer, F. A. J. L. Circadian misalignment
507 increases cardiovascular disease risk factors in humans. *Proc Natl Acad Sci U*
508 *S A* **113**, E1402-1411 (2016). https://doi.org/10.1073/pnas.1516953113
509 8 Haspel, J. A. *et al.* Perfect timing: circadian rhythms, sleep, and immunity - an
510 NIH workshop summary. *JCI Insight* **5**, e131487,-131487 (2020).
511 https://doi.org/10.1172/jci.insight.131487
512 9 Scheiermann, C., Kunisaki, Y. & Frenette, P. S. Circadian control of the immune
513 system. *Nat Rev Immunol* **13**, 190-198 (2013). https://doi.org/10.1038/nri3386
514 10 Jerigova, V., Zeman, M. & Okuliarova, M. Circadian Disruption and
515 Consequences on Innate Immunity and Inflammatory Response. *Int J Mol Sci*
516 **23** (2022). https://doi.org/10.3390/ijms232213722
517 11 Curtis, A. M., Bellet, M. M., Sassone-Corsi, P. & O'Neill, L. A. Circadian clock
518 proteins and immunity. *Immunity* **40**, 178-186 (2014).
519 https://doi.org/10.1016/j.immuni.2014.02.002
520 12 Rijo-Ferreira, F. & Takahashi, J. S. Circadian rhythms in infectious diseases
521 and symbiosis. *Semin Cell Dev Biol* **126**, 37-44 (2022).
522 https://doi.org/10.1016/j.semcdb.2021.09.004
523 13 Lowy, F. D. Staphylococcus aureus Infections. *New England Journal of*
524 *Medicine* **339**, 520-532 (1998).
525 https://doi.org/10.1056/NEJM199808203390806
526 14 David, M. Z. & Daum, R. S. Community-associated methicillin-resistant
527 Staphylococcus aureus: epidemiology and clinical consequences of an
528 emerging epidemic. *Clin Microbiol Rev* **23**, 616-687 (2010).
529 https://doi.org/10.1128/CMR.00081-09
530 15 Moldovan, A. & Fraunholz, M. J. In or out: Phagosomal escape of
531 Staphylococcus aureus. *Cell Microbiol* **21**, e12997 (2019).
532 https://doi.org/10.1111/cmi.12997
533 16 Watkins, K. E. & Unnikrishnan, M. Evasion of host defenses by intracellular
534 Staphylococcus aureus. *Adv Appl Microbiol* **112**, 105-141 (2020).
535 https://doi.org/10.1016/bs.aambs.2020.05.001
536 17 Marro, F. C. *et al.* In vitro antibiotic activity against intraosteoblastic
537 Staphylococcus aureus: a narrative review of the literature. *J Antimicrob*
538 *Chemother* **76**, 3091-3102 (2021). https://doi.org/10.1093/jac/dkab301

18 Peyrusson, F. *et al.* Intracellular Staphylococcus aureus persisters upon antibiotic exposure. *Nat Commun* **11**, 2200 (2020). https://doi.org/10.1038/s41467-020-15966-7

19 Tsujihana, K. *et al.* Circadian protection against bacterial skin infection by epidermal CXCL14-mediated innate immunity. *Proc Natl Acad Sci U S A* **119**, e2116027119 (2022). https://doi.org/10.1073/pnas.2116027119

20 Balsalobre, A., Marcacci, L. & Schibler, U. Multiple signaling pathways elicit circadian gene expression in cultured Rat-1 fibroblasts. *Curr Biol* **10**, 1291-1294 (2000). https://doi.org/10.1016/s0960-9822(00)00758-2

21 Yagita, K. & Okamura, H. Forskolin induces circadian gene expression of rPer1, rPer2 and dbp in mammalian rat-1 fibroblasts. *FEBS Lett* **465**, 79-82 (2000). https://doi.org/10.1016/s0014-5793(99)01724-x

22 Maier, B., Lorenzen, S., Finger, A. M., Herzel, H. & Kramer, A. Searching Novel Clock Genes Using RNAi-Based Screening. *Methods Mol Biol* **2130**, 103-114 (2021). https://doi.org/10.1007/978-1-0716-0381-9_8

23 Zhang, Y. *et al.* Dosing time dependent in vitro pharmacodynamics of Everolimus despite a defective circadian clock. *Cell Cycle* **17**, 33-42 (2018). https://doi.org/10.1080/15384101.2017.1387695

24 Mastrullo, V. *et al.* Pericytes' Circadian Clock Affects Endothelial Cells' Synchronization and Angiogenesis in a 3D Tissue Engineered Scaffold. *Front Pharmacol* **13**, 867070 (2022). https://doi.org/10.3389/fphar.2022.867070

25 Torre, D., Lachmann, A. & Ma'ayan, A. BioJupies: Automated Generation of Interactive Notebooks for RNA-Seq Data Analysis in the Cloud. *Cell Syst* **7**, 556-561 e553 (2018). https://doi.org/10.1016/j.cels.2018.10.007

26 Ge, S. X., Son, E. W. & Yao, R. iDEP: an integrated web application for differential expression and pathway analysis of RNA-Seq data. *BMC Bioinformatics* **19**, 534 (2018). https://doi.org/10.1186/s12859-018-2486-6

27 Kim, S. Y. & Volsky, D. J. PAGE: parametric analysis of gene set enrichment. *BMC Bioinformatics* **6**, 144 (2005). https://doi.org/10.1186/1471-2105-6-144

28 Bunger, M. K. *et al.* Mop3 is an essential component of the master circadian pacemaker in mammals. *Cell* **103**, 1009-1017 (2000). https://doi.org/10.1016/s0092-8674(00)00205-1

29 Niemann, S. *et al.* Correction for Niemann et al., "More Is Not Always Better-the Double-Headed Role of Fibronectin in Staphylococcus aureus Host Cell Invasion". *mBio* **14**, e0292123 (2023). https://doi.org/10.1128/mbio.02921-23

30 Sinha, B. *et al.* Fibronectin-binding protein acts as Staphylococcus aureus invasin via fibronectin bridging to integrin alpha5beta1. *Cell Microbiol* **1**, 101-117 (1999). https://doi.org/10.1046/j.1462-5822.1999.00011.x

31 Zhou, T.-T. *et al.* Monoclonal antibody against I-lectin module of SraP blocks adhesion and protects mice against Staphylococcus aureus challenge. *Journal of Microbiology, Immunology and Infection* **54**, 420-428 (2021). https://doi.org/10.1016/j.jmii.2019.08.019

32 Kukita, K. *et al.* Staphylococcus aureus SasA is responsible for binding to the salivary agglutinin gp340, derived from human saliva. *Infection and Immunity* **81**, 1870-1879 (2013). https://doi.org/10.1128/IAI.00011-13

33 Yang, Y. H. *et al.* Structural insights into SraP-mediated Staphylococcus aureus adhesion to host cells. *PLoS Pathog* **10**, e1004169 (2014). https://doi.org/10.1371/journal.ppat.1004169

34 Arjona, A. & Sarkar, D. K. Are circadian rhythms the code of hypothalamic-immune communication? Insights from natural killer cells. *Neurochem Res* **33**, 708-718 (2008). https://doi.org/10.1007/s11064-007-9501-z

35 Tognini, P., Thaiss, C. A., Elinav, E. & Sassone-Corsi, P. Circadian Coordination of Antimicrobial Responses. *Cell Host Microbe* **22**, 185-192 (2017). https://doi.org/10.1016/j.chom.2017.07.007

36 Abe, Y. O. *et al.* Rhythmic transcription of Bmal1 stabilizes the circadian timekeeping system in mammals. *Nature Communications* **13**, 4652 (2022). https://doi.org/10.1038/s41467-022-32326-9

37 Zhuang, X. *et al.* The circadian clock components BMAL1 and REV-ERBα regulate flavivirus replication. *Nature Communications* **10** (2019). https://doi.org/10.1038/s41467-019-08299-7

38 Zhuang, X. *et al.* The circadian clock component BMAL1 regulates SARS-CoV-2 entry and replication in lung epithelial cells. *iScience* **24**, 103144 (2021). https://doi.org/10.1016/j.isci.2021.103144

39 Kitchen, G. B. *et al.* The clock gene Bmal1 inhibits macrophage motility, phagocytosis, and impairs defense against pneumonia. *Proc Natl Acad Sci U S A* **117**, 1543-1551 (2020). https://doi.org/10.1073/pnas.1915932117

40 Keller, M. *et al.* A circadian clock in macrophages controls inflammatory immune responses. *Proc Natl Acad Sci U S A* **106**, 21407-21412 (2009). https://doi.org/10.1073/pnas.0906361106

41 Josse, J., Laurent, F. & Diot, A. Staphylococcal Adhesion and Host Cell Invasion: Fibronectin-Binding and Other Mechanisms. *Front Microbiol* **8**, 2433 (2017). https://doi.org/10.3389/fmicb.2017.02433

42 Massey, R. C. *et al.* Fibronectin-binding protein A of Staphylococcus aureus has multiple, substituting, binding regions that mediate adherence to fibronectin and invasion of endothelial cells. *Cell Microbiol* **3**, 839-851 (2001). https://doi.org/10.1046/j.1462-5822.2001.00157.x

43 Askarian, F. *et al.* The interaction between Staphylococcus aureus SdrD and desmoglein 1 is important for adhesion to host cells. *Sci Rep* **6**, 22134 (2016). https://doi.org/10.1038/srep22134

44 Geoghegan, J. A. *et al.* Molecular characterization of the interaction of staphylococcal microbial surface components recognizing adhesive matrix molecules (MSCRAMM) ClfA and Fbl with fibrinogen. *J Biol Chem* **285**, 6208-6216 (2010). https://doi.org/10.1074/jbc.M109.062208

45 Hirschhausen, N. *et al.* A novel staphylococcal internalization mechanism involves the major autolysin Atl and heat shock cognate protein Hsc70 as host cell receptor. *Cell Microbiol* **12**, 1746-1764 (2010). https://doi.org/10.1111/j.1462-5822.2010.01506.x

46 Sun, H., Li, R. W., Wang, T. T. Y. & Ding, L. The Ligand Binding Domain of the Cell Wall Protein SraP Modulates Macrophage Apoptosis and Inflammatory Responses in Staphylococcus aureus Infections. *Molecules* **30** (2025). https://doi.org/10.3390/molecules30051168

47 Lee, Y., Field, J. M. & Sehgal, A. Circadian Rhythms, Disease and Chronotherapy. *J Biol Rhythms* **36**, 503-531 (2021). https://doi.org/10.1177/07487304211044301

634 **Supplementary figure legends**

635 **Figure S1. Bacterial growth kinetics is delayed at 24 h compared to 12 h after**
636 **synchronisation.** (A) A549 epithelial cells were synchronized with FSK every 6 h over
637 a 24 h period and infected with *S. aureus* for 1 h, extracellular bacteria were removed
638 by gentamycin/lysostaphin treatment and cells imaged in presence of lysostaphin for
639 12 hours. (B) Average number of intracellular *S. aureus* foci in hourly intervals ± SD.

640

641 **Figure S2. Validating the *BMAL1* knockdown in A549 lung epithelial cells.** (A)
642 Generation of stable *shBMAL1* cell line expressing puromycin and eGFP. (B)
643 Quantification of knockdown efficiency from RNA-Seq experiment. (C) Heatmap of
644 Circadian Rhythm KEGG pathway from PGSEA was significantly deregulated (N=3,
645 condition and cell line).

646

647 **Figure S3. Comparison of the invasion of *S. aureus* JE2 and transposon mutants**
648 **of *fnbA* and *fnbB* and genes.** Parental and *shBMAL1* A549 cells were infected with
649 JE2 *S. aureus WT* and mutant strains of *S. aureus f*or 1 hour and intracellular bacteria
650 quantified by colony counts. (A) Bacterial counts (CFU) after 1 h infection (B) Fold
651 change in CFU calculated with respect to JE2 strain. Statistical significance of 2-way
652 ANOVA with Sidac post-hoc test as **** $p<0.0001$.

653

654